Synthesis and Characterization of Palladium Complexes Containing Tridentate Ligands with PXP (X = C, N, O, S, As) Donor Sets and Their Evaluation as Electrochemical CO_2 Reduction Catalysts

Bryan D. Steffey, Alex Miedaner, Mary L. Maciejewski-Farmer, Paul R. Bernatis, Andrew M. Herring, Viloya S. Allured,† Vasili Carperos,† and Daniel L. DuBois*

National Renewable Energy Laboratory, Golden, Colorado 80401

Received May 18, 1994®

Square-planar palladium complexes containing tridentate ligands with PXP (X = C, N, O, S, and As) donor sets have been prepared. For $[Pd(POP\text{-}R)(CH_3CN)_2](BF_4)_2$ complexes (where POP-R is bis((diethylphosphino)ethyl) ether, bis((diphenylphosphino)ethyl) ether, or bis((dicyclohexylphosphino)ethyl) ether), the POP-R ligands function as bidentate ligands. For all other complexes, the PXP ligands function as tridentate ligands. The complex $[Pd(PCP)(PEt_3)](BF_4)$ (where PCP is 2,6-bis((diphenylphosphino)methyl)phenyl) crystallizes in the triclinic space group $P\bar{1}$ with a = 10.276(2) Å, b = 10.978(2) Å, c = 18.807(3) Å, α = 84.820(10)°, β = 76.910(10)°, γ = 63.870(10)°, V = 1855.2(6) Å^3, and Z = 2. The structure was refined to R = 0.0335 and R_w = 0.0442 for 7570 independent reflections with $F > 4.0\sigma(F)$. $[Pd(PNP)(PEt_3)](BF_4)_2$ (where PNP is 2,6-bis((diphenylphosphino)methyl)pyridine) crystallizes in the monoclinic space group $C2/c$ with a = 13.246(2) Å, b = 14.299(2) Å, c = 20.847(4) Å, β = 100.96(2)°, V = 3876.5(11) Å^3, and Z = 4. The structure was refined to R = 0.0436 and R_w = 0.0556 for 3106 independent reflections with $F > 6.0\sigma(F)$. Both cations adopt square-planar structures with small C–Pd–P (79.0 and 79.1°) and N–Pd–P (80.3°) chelate angles. The Pd–P bond distances of the triethylphosphine ligands differ by 0.079 Å for these two complexes. The acetonitrile complexes undergo one-electron reductions, while the corresponding triethylphosphine complexes undergo two-electron reductions. $[Pd(PCP)(CH_3CN)](BF_4)$ exhibits significant catalytic currents in the presence of acid and CO_2. The dependence of the catalytic current on CO_2 and acid concentrations is consistent with the formation of a hydroxycarbonyl intermediate which decomposes in the presence of acid to form H_2 as the catalytic product. Structure–activity relationships for CO_2 reduction for this class of compounds are discussed.

Introduction

The electrochemical reduction of CO_2 is catalyzed by a variety of homogeneous and heterogeneous catalysts.[1] The most extensively studied homogeneous catalysts are transition-metal complexes containing either macrocyclic or bipyridine ligands.[2] Only a few reports have appeared describing the electrochemical reduction of CO_2 using transition-metal phosphine complexes.[3–7] As a result of studies of transition-metal complexes containing polyphosphine ligands, $[Pd(triphosphine)(solvent)](BF_4)_2$ complexes were found to catalyze the electrochemical reduction of CO_2 to CO in acidic dimethylformamide or acetonitrile solutions.[4,6,8] Depending on the nature of the triphosphine ligand, these complexes can exhibit high catalytic rates and selectivities at relatively positive potentials. Palladium complexes in which the terminal phosphorus atoms have been substituted with nitrogen or sulfur atoms failed to catalyze the electrochemical reduction of CO_2 to CO.[6] In this paper we report the synthesis of palladium complexes containing tridentate ligands with PCP, PNP, POP, PSP, and PAsP donor sets to determine the effect of varying the identity of the central donor atom of the tridentate ligand on catalytic activity. None of the complexes prepared catalyze the electrochemical reduction of CO_2 under conditions where the analogous triphosphine complexes exhibit significant activity. However, an enhanced rate of proton reduction in the presence of CO_2 for some of the complexes indicates that CO_2 intermediates are formed upon reduction.

Experimental Section

Materials and Physical Methods. Reagent-grade diethyl ether, tetrahydrofuran (THF), and toluene were purified by

† Department of Chemistry and Biochemistry, University of Colorado, Boulder, CO 80309.

® Abstract published in *Advance ACS Abstracts,* November 1, 1994.

(1) *Electrochemical and Electrocatalytic Reactions of Carbon Dioxide*; Sullivan, B. P., Krist, K., Guard, H. E., Eds.; Elsevier: New York, 1993. *Proceedings of the International Symposium on Chemical Fixation of Carbon Dioxide*, Nagoya, Japan, Dec. 2–4, 1991. *Catalytic Activation of Carbon Dioxide*; ACS Symposium Series 363; Ayers, W. M., Ed.; American Chemical Society: Washington, DC, 1988.

(2) Collin, J.-P.; Sauvage, J.-P. *Coord. Chem. Rev.* **1989**, *93*, 245.

(3) Slater, S.; Wagenknecht, J. H. *J. Am. Chem. Soc.* **1984**, *106*, 5367.

(4) DuBois, D. L.; Miedaner, A. *J. Am. Chem. Soc.* **1987**, *109*, 113.

(5) Szymaszek, A.; Pruchnik, F. P. *J. Organomet. Chem.* **1987**, *376*, 133.

(6) DuBois, D. L.; Miedaner, A.; Haltiwanger, R. C. *J. Am. Chem. Soc.* **1991**, *113*, 8753.

(7) Ratliff, K. S.; Lentz, R. E.; Kubiak, C. P. *Organometallics* **1992**, *11*, 1986.

(8) DuBois, D. L.; Miedaner, A. *Inorg. Chem.* **1986**, *25*, 4642; **1988**, *27*, 2479. Miedaner, A.; DuBois, D. L.; Curtis, C. J. *Organometallics* **1993**, *12*, 299.

0276-7333/94/2313-4844$04.50/0

distillation from sodium benzophenone ketyl. Acetonitrile and dichloromethane were distilled from CaH_2 under nitrogen. Reagent-grade ethanol and dimethylformamide from Burdick and Jackson were deoxygenated by purging with nitrogen prior to use. Dimethylformamide was stored in an inert-atmosphere glovebox after deoxygenation, and ethanol was stored under a positive pressure of nitrogen in a flask. Dichloromethane-d_2 and acetonitrile-d_3 were purified by vacuum transfer from CaH_2 and stored in a glovebox. Acetone-d_6 was dried over 4-Å molecular sieves, vacuum-transferred, and stored in a glovebox. Diphenylphosphine and triethylphosphine were obtained from Strem Chemicals, Inc., and used without further purification. Vinylmagnesium bromide in THF and potassium *tert*-butoxide (KO-*t*-Bu) were obtained from Aldrich Chemical Co., Inc. KO-*t*-Bu was sublimed prior to use. Phenylarsine oxide was purchased from Alfa/Johnson Matthey.

NMR spectra were obtained on a Varian Unity 300-MHz NMR spectrometer operating at 299.95, 121.42, and 75.43 MHz for ^1H, ^{31}P, and ^{13}C nuclei, respectively. Chemical shifts for ^1H NMR spectra are reported in ppm relative to tetramethylsilane using solvent peaks as secondary references. ^{31}P NMR chemical shifts are referenced to external H_3PO_4. Infrared spectra were obtained using a Nicolet 510 P spectrometer on samples prepared as Nujol mulls or dichloromethane solutions. IR spectra on solutions at elevated CO pressures as specified in the text were made using a commercially available high-pressure cell (Harrick Scientific Corp.). Coulometric measurements were carried out at 25–30 °C using a Princeton Applied Research Model 173 potentiostat equipped with a Model 179 digital coulometer and a Model 175 universal programmer. The working electrode was constructed from a reticulated vitreous carbon rod with a 1-cm diameter and length of 2.5 cm (100 pores/in., The Electrosynthesis Co., Inc.). The counter electrode was a W wire, and a Pt wire immersed in a 50:50 mixture of permethylferrocene/permethylferrocenium was used as a reference electrode.[9] The electrode compartments were separated by Vycor disks (7-mm diameter). Measurements of current efficiencies for gas production were carried out in a sealed flask (120 mL), from which gas aliquots were withdrawn for gas chromatographic analysis. Details of chromatography conditions are presented elsewhere.[4] In a typical experiment, a 1.0×10^{-3} M solution of catalyst in dimethylformamide (10.0 mL) was saturated with CO_2 by purging the solution for 30 min. H_3PO_4 (20 μL of a 14.7 M solution for [Pd(PCP)(CH_3CN)](BF_4)) or HBF_4 (50 μL of a 9.4 M aqueous solution for all other complexes) was added via syringe, and the solution was electrolyzed at potentials approximately 100 mV negative of the peak potential of the first cathodic wave of the complex. The electrolyses were considered complete when the current had decayed to 5–10% of the initial value. Cyclic voltammetry and chronoamperometry experiments were carried out using a Cypress Systems computer-aided electrolysis system. The working electrode was a glassy-carbon disk of 1-mm diameter. The counter electrode was a glassy-carbon rod, and the reference electrode was a Pt wire immersed in a permethylferrocene/permethylferrocenium solution.[9] Ferrocene was used as an internal standard, and all potentials are reported vs the ferrocene/ferrocenium couple.[10] All solutions for cyclic voltammetry and coulometric experiments were 0.3 N NEt_4BF_4 in dimethylformamide or acetonitrile. Catalytic currents were measured on solutions containing H_3PO_4 as the acid for [Pd(PCP)(CH_3CN)](BF_4) and HBF_4 (0.05 M) for the remaining complexes.

X-ray crystallographic measurements were carried out on a Siemens P3/F autodiffractometer. Mo Kα radiation (monochromatized by diffraction off a highly oriented graphite crystal) was used in this study. The crystals were mounted with epoxy on glass fibers. Programs in the Siemens X-ray package were used for data collection and for structure solution and refinement. Details of the experimental conditions are given in the supplementary material. Table 1 summarizes the crystal data for [Pd(PCP)(PEt_3)](BF_4) and [Pd(PNP)(PEt_3)](BF_4)$_2$.

Table 1. Crystal Data, Data Collection Conditions, and Solution and Refinement Details

	[Pd(PCP)(PEt_3)](BF_4)	[Pd(PNP)(PEt_3)](BF_4)$_2$
empirical formula	$C_{38}H_{42}BF_4P_3Pd$	$C_{37}H_{42}B_2F_8NP_3Pd$
color, habit	clear, rectangular prism	clear, colorless rhombohedron
crystal dimensions	0.3 × 0.6 × 0.7 mm	0.2 × 0.1 × 0.75 mm
space group	$P\bar{1}$	$C2/c$
crystal system	triclinic	monoclinic
unit cell dimensions		
a	10.276(2) Å	13.246(2) Å
b	10.978(2) Å	14.299(2) Å
c	18.807(3) Å	20.847(4) Å
α	84.820(10)°	
β	76.910(10)°	100.96(2)°
γ	63.870(10)°	
V	1855.2(6) Å^3	3876.5(11) Å^3
Z	2	4
d_{calc}	1.405 g/cm^3	1.497 g/cm^3
formula weight	784.8	873.6 amu
absorption coefficient	0.665 mm^{-1}	0.658 mm^{-1}
radiation	Mo Kα (λ = 0.710 73 Å)	Mo Kα (λ = 0.710 73 Å)
temp, °C	22–24	22–24
final residuals (obsd data)	R = 3.35%, R_w = 4.42%	R = 4.36%, R_w = 5.56%
residuals (all data)	R = 3.88%, R_w = 4.53%	R = 6.49%, R_w = 6.23%

Syntheses. The compounds 1,3-bis((diphenylphosphino)methyl)benzene,[11] 2,6-bis((diphenylphosphino)methyl)pyridine (PNP),[12] bis((diphenylphosphino)ethyl)amine (PNHP),[13,14] dichlorophenylarsine,[15] bis((diphenylphosphino)ethyl) sulfide (PSP),[16] bis((diphenylphosphino)ethyl) ether (POP),[17] and [Pd($CH_3CN)_4$](BF_4)$_2$[18] were prepared by literature methods. Slight modifications of the literature method for POP were used to prepare the ethyl and cyclohexyl analogues. ^1H NMR spectral data for all new ligands are listed below. ^{31}P NMR data for both ligands and complexes are summarized in Table 2.

Bis((diethylphosphino)ethyl) Ether (POP-E). ^1H NMR (CD_3CN): OCH_2CH_2P, 3.51 ppm (dt, $^3J_{HH}$ = 7.5 Hz, $^3J_{PH}$ = 8.4 Hz); OCH_2CH_2P, 1.62 ppm (dt, $^2J_{PH}$ = 1.5 Hz); PCH_2CH_3, 1.40 ppm (q, $^3J_{HH}$ = 6.9 Hz, $^2J_{PH}$ < 1 Hz); PCH_2CH_3, 0.95 ppm (dt, $^3J_{PH}$ = 14.7 Hz).

Bis((dicyclohexylphosphino)ethyl) Ether (POP-C). ^1H NMR (toluene-d_8): OCH_2CH_2P, 3.67 ppm (dt, $^3J_{HH}$ = 8 Hz, $^3J_{PH}$ = 6 Hz); OCH_2CH_2P, 1.80 ppm (dt, $^2J_{PH}$ = 3 Hz); C_6H_{11}, 1.1–1.75 ppm (m's).

Divinylphenylarsine. A solution of vinylmagnesium bromide (22 mmol) in THF (22 mL) was added to a cold solution (−78 °C) of phenyldichloroarsine (2.0 g, 8.97 mmol) in THF (75 mL). The solution was warmed to room temperature and stirred overnight. The THF was removed from the solution by distillation at atmospheric pressure; then divinylphenylarsine (0.62 g, 35%) was distilled at 70 °C and 0.2 Torr. ^1H NMR (toluene-d_8): Ph, 7.0–7.2, 7.4–7.5 ppm (m's); $AsCH$=CH_2,

(9) Bashkin, J. K.; Kinlen, P. *Inorg. Chem.* **1990**, *29*, 4507.
(10) Gagne, R. R.; Koval, C. A.; Lisensky, G. C. *Inorg. Chem.* **1980**, *19*, 2855. Gritzner, G.; Kuta, J. *Pure Appl. Chem.* **1984**, *56*, 461. Hupp, J. T. *Inorg. Chem.* **1990**, *29*, 5010.
(11) Rimml, H.; Venanzi, L. M. *J. Organomet. Chem.* **1983**, *259*, C6. For other complexes of this type see: Moulton, C. J.; Shaw, B. C. *J. Chem. Soc., Dalton Trans.* **1976**, 1020. Kaska, W. C.; Nemeh, S.; Shirazi, A.; Potuznik, S. *Organometallics* **1988**, *7*, 13. Haenel, M. W.; Jakubik, D.; Kruger, C.; Betz, P. *Chem. Ber.* **1991**, *124*, 333.
(12) Dahlhoff, W. V.; Nelson, S. M. *J. Chem. Soc. A* **1971**, 2184.
(13) Nuzzo, R. G.; Haynie, S. L.; Wilson, M. E.; Whitesides, G. M. *J. Org. Chem.* **1981**, *46*, 2861.
(14) Sacconi, L.; Morassi, R. *J. Chem. Soc. A* **1968**, 2997.
(15) Millar, I. T.; Heaney, H.; Heinekey, D. M.; Fernelius, W. C. *Inorg. Synth.* **1960**, *6*, 113. Levason, W.; McAuliffe, C. A. *Ibid.* **1976**, *16*, 184.
(16) Degischer, G.; Schwarzenbach, G. *Helv. Chim. Acta* **1966**, *49*, 1927.
(17) Sacconi, L.; Gelsomini, J. *Inorg. Chem.* **1968**, *7*, 291.
(18) Sen, A.; Ta-Wang, L. *J. Am. Chem. Soc.* **1981**, *103*, 4627. Hathaway, B. J.; Holah, D. G.; Underhill, A. E. *J. Chem. Soc.* **1962**, 2444.

Table 2. ^{31}P NMR Data for Ligands and Complexes

compound	PR_2 (ppm)[a]	PEt_3 (ppm)	J (Hz)	ΔC (ppm)[b]
PCP	−8.8			0
[Pd(PCP)(CH_3CN)](BF_4), **1**	43.2			52
[Pd(PCP)(PEt_3)](BF_4), **2**	48.1 (d)	7.7 (t)	37	57
PNP	−4.4			0
[Pd(PNP)(CH_3CN)](BF_4)$_2$, **3**	38.0			42
{[Pd(PNP)]$_2$(μ-PNP)}(BF_4)$_4$, **4**	41.4 (d)	21.9 (t, PPh_2)	18	46
[Pd(PNP)(PEt_3)](BF_4)$_2$, **5**	41.4 (d)	28.5 (t)	18	46
PNHP	−13.1			0
[Pd(PNHP)(CH_3CN)](BF_4)$_2$, **6**	47.5			61
[Pd(PNHP)(PEt_3)](BF_4)$_2$, **9**	47.6 (d)	22.8 (t)	24	61
PSP	−16.4			0
[Pd(PSP)(CH_3CN)](BF_4)$_2$, **7**	55.3			72
[Pd(PSP)(PEt_3)](BF_4)$_2$	50.6 (d)	26.0 (t)	21	67
PAsP	−12.4			0
[Pd(PAsP)(CH_3CN)](BF_4)$_2$, **8**	57.6			70
[Pd(PAsP)(PEt_3)](BF_4)$_2$	59.5 (d)	18.6 (t)	27	72
POP-E	−26.2			0
[Pd(POP-E)(CH_3CN)$_2$](BF_4)$_2$, **10a**	36.2			62
[Pd(POP-E)(PEt_3)](BF_4)$_2$, **11a**	47.2 (d)	41.6 (t)	20	73
POP	−15.2			0
[Pd(POP)(CH_3CN)$_2$](BF_4)$_2$, **10b**	19.8			35
[Pd(POP)(PEt_3)](BF_4)$_2$, **11b**	44.8 (d)	40.4 (t)	17	60
POP-C	−4.9			0
cis-[Pd(POP-C)(CH_3CN)$_2$)](BF_4)$_2$, **10c**	52.1			57
trans-[Pd(POP-C)(CH_3CN)](BF_4)$_2$, **10c**	71			76
[Pd(POP-C)(PEt_3)](BF_4)$_2$, **11c**	61.4 (d)	36.8 (t)	19	66
etp	−12.8 (d)			0
[Pd(etp)(CH_3CN)](BF_4)$_2$[c]	54.6 (d)			67
[Pd(etp)(PEt_3)](BF_4)$_2$[c]	54.4 (dd)	11.3 (dt)	29	67
ttp	−18			0
[Pd(ttp)(CH_3CN)](BF_4)$_2$[c]	−5.2			13
[Pd(ttp)(PEt_3)](BF_4)$_2$[c]	2.0	−17.2 (dt)	42	19

[a] All spectra were recorded in acetonitrile-d_3 except for the last entry, which was recorded in nitromethane-d_3. Chemical shifts are given in ppm relative to external H_3PO_4. [b] ΔC is the coordination chemical shift and is the difference in the chemical shift between the free ligand and the corresponding resonance for the complex. [c] Data from ref 6.

6.49 ppm (dd, $^3J_{HH}$(trans) = 19 Hz, $^3J_{HH}$(cis) = 11 Hz); AsCH=CH_2 (trans to As), 5.78 ppm (d); AsCH=CH_2 (cis to As), 5.61 ppm (d).

Bis((diphenylphosphino)ethyl)phenylarsine (PAsP). Divinylphenylarsine (0.50 g, 2.43 mmol), diphenylphosphine (1.0 g, 5.4 mmol), and potassium *tert*-butoxide (0.1 g) were dissolved in THF (25 mL). After the solution was refluxed for 1 week, the solvent was removed on a vacuum line to yield a colorless oil (1.50 g, 97%). ^{1}H NMR (toluene-d_8): Ph, 6.9−7.3 ppm (m's); AsCH_2CH_2P, 1.6−1.8, 2.0−2.2 ppm (m's).

[Pd(PCP)(CH_3CN)](BF_4) (1). A solution of 1,3-bis((diphenylphosphino)methyl)benzene (0.47 g, 1.0 mmol) in THF (3.5 mL) was added to a solution of [Pd(CH_3CN)$_4$](BF_4)$_2$ (0.44 g, 1.0 mmol) in acetonitrile (40 mL). The reaction mixture was stirred at 50 °C for 0.5 h. A yellow solid resulted when the solvent was removed by applying a vacuum. The product was recrystallized twice. The first recrystallization was from a mixture of dichloromethane and ethanol, and the second was from acetone by slow evaporation of the solvent under nitrogen. The white needles that formed were collected by filtration and dried in a vacuum (0.30 g, 42%). Anal. Calcd for $C_{34}H_{30}BF_4NP_2Pd$: C, 57.70; H, 4.27; N, 1.98. Found: C, 58.33; H, 4.28; N, 1.92. ^{1}H NMR (acetone-d_6): Ph, 7.05−7.8 ppm; CH_2PPh$_2$, 4.25 ppm (t, splitting 4.9 Hz); CH_3CN, 2.21 ppm (s). IR (CH_2Cl_2): ν_{CN}, 2287 and 2316 cm^{-1}.

[Pd(PCP)(PEt_3)](BF_4) (2). A solution of PCP (0.47 g, 1.0 mmol) in THF (3.5 mL) was added to a solution of [Pd(CH_3CN)$_4$](BF_4)$_2$ (0.44 g, 1.0 mmol) in acetonitrile (30 mL). The yellow reaction mixture was stirred overnight at room temperature, and then triethylphosphine (0.12 g, 1 mmol) was added. After the solution was stirred for an additional 2 h, the solvent was removed on a vacuum line to produce a yellow powder. The product was recrystallized from a mixture of dichloromethane and ethanol to produce a white solid. The product was collected by filtration and dried in a vacuum (0.50 g, 64%). Anal. Calcd for $C_{38}H_{42}BF_4P_3Pd$: C, 58.15; H, 5.40; P, 11.85. Found: C, 58.64; H, 5.50; P, 11.33. ^{1}H NMR (CD_3CN): Ph, 7.0−7.8 ppm (m); CH_2PPh$_2$, 4.30 ppm (t, splitting 4.5 Hz); PCH_2CH$_3$, 0.96 ppm (quintet, $^2J_{PH}$ = $^3J_{HH}$ = 8 Hz); PCH$_2$CH_3, 0.76 ppm (d of t, $^3J_{PH}$ = 17 Hz).

[Pd(PNP)(CH_3CN)](BF_4)$_2$ (3) and {[Pd(PNP)]$_2$(μ-PNP)}(BF_4)$_4$ (4). A solution of [Pd(CH_3CN)$_4$](BF_4)$_2$ (0.44 g, 1.0 mmol) in acetonitrile (30 mL) was added to a solution of 2,6-bis((diphenylphosphino)methyl)pyridine (PNP; 0.48 g, 1.0 mmol) in dichloromethane (50 mL). The reaction mixture was stirred for 1 h at room temperature. Then the solvent was removed on a vacuum line to produce a yellow solid. ^{31}P and ^{1}H NMR data of this solid dissolved in CD_3CN are discussed in the text. These spectra indicate a mixture of [Pd(PNP)(CH_3CN)](BF_4)$_2$ and {[Pd(PNP)]$_2$(μ-PNP)}(BF_4)$_4$.

[Pd(PNP)(PEt_3)](BF_4)$_2$ (5). Triethylphosphine (0.16 g, 1.25 mmol) was added to an acetone solution (40 mL) of the solid mixture resulting from the previous preparation. The solution was allowed to stand for 1 day, during which well-shaped crystals formed. The crystals were collected by filtration and dried in a vacuum (0.54 g, 64%). Anal. Calcd for $C_{37}H_{42}B_2F_8NP_3Pd$: C, 50.87; H, 4.85; N, 1.60. Found: C, 51.10; H, 4.75; N, 1.65. ^{1}H NMR (CD_3CN): phenyl and pyridine protons, 7−8 ppm (m); CH_2PPh$_2$, 4.87 ppm (t, splitting 5.1 Hz); PCH_2CH$_3$, 1.32 ppm (quintet, $^2J_{PH}$ = $^3J_{HH}$ = 8 Hz); PCH$_2$CH_3, 0.85 ppm (dt, $^3J_{PH}$ = 19 Hz).

[Pd(PNHP)(CH_3CN)](BF_4)$_2$ (6). A solution of bis((diphenylphosphino)ethyl)amine (PNHP) (0.81 g, 1.83 mmol) in dichloromethane (30 mL) was added to a solution of [Pd(CH_3CN)$_4$](BF_4)$_2$ (0.81 g, 1.83 mmol) in acetonitrile (30 mL). The reaction mixture was stirred for 5 days at room temperature. The solvent was removed on a vacuum line to produce a white solid (1.20 g, 87%), which was pure on the basis of ^{31}P and ^{1}H NMR data. An analytical sample was recrystallized from a mixture of dichloromethane and ethanol containing 2% CH_3CN. Anal. Calcd for $C_{30}H_{32}B_2F_8N_2P_2Pd$: C, 47.25; H, 4.23; N, 3.67. Found: C, 47.33; H, 4.03; N, 3.63. ^{1}H NMR (acetone-d_6): Ph, 7.5−8.2 ppm (m); NH, 6.9 ppm (broad singlet); NCH_2CH_2P, 2.9−3.8 ppm (m); CH_3CN, 2.61 ppm (s). IR (CH_2Cl_2): ν_{CN}, 2305 cm^{-1}; ν_{NH}, 3189 cm^{-1}.

[Pd(PNHP)(PEt_3)](BF_4)$_2$ (9). Triethylphosphine (0.08 g, 0.66 mmol) was added via syringe to a stirred solution of [Pd(PNHP)(CH_3CN)](BF_4)$_2$ (0.50 g, 0.66 mmol) in CH_3CN (50 mL). After 2 h at room temperature, the solvent was removed with a vacuum line to produce a white solid. The product (0.33 g, 60%) was recrystallized from a mixture of acetone and hexanes. Anal. Calcd for $C_{34}H_{54}B_2F_8NP_3Pd$: C, 48.62; H, 5.28; N, 1.67; P, 11.07. Found: C, 48.79; H, 4.75; N, 1.63; P, 10.83. ^{1}H NMR (CD_3CN): Ph, 7.6−8.2 ppm (m); NH, 5.8 ppm (broad singlet); NCH_2CH_2P, 2.4−3.6 ppm (m); PCH_2CH$_3$, 1.24 ppm (quintet, $^3J_{HH}$ = $^2J_{PH}$ = 8 Hz); PCH$_2$CH_3, 0.72 ppm (dt, $^3J_{PH}$ = 18 Hz). IR (CH_2Cl_2): ν_{NH}, 3204 cm^{-1}.

[Pd(POP-E)(CH_3CN)$_2$](BF_4)$_2$ (10a). [Pd(CH_3CN)$_4$](BF_4)$_2$ (0.88 g, 2.0 mmol) was added to a solution of bis((diethylphosphino)ethyl) ether (POP-E; 0.50 g, 2.0 mmol) in acetonitrile (20 mL). The yellow solution was stirred overnight at room temperature. Solvent was removed with a vacuum line until the volume of the solution was approximately 5 mL. Ether (30 mL) was added to the concentrated solution, which was placed in a refrigerator (4 °C) overnight. The yellow solid that precipitated was collected by filtration and dried in a vacuum (1.08 g, 95%). An analytical sample was recrystallized from a mixture of acetonitrile and ether. Anal. Calcd for $C_{16}H_{34}B_2F_8N_2PdP_2O$: C, 31.38; H, 5.60; N, 4.57; F, 24.82. Found: C, 31.46; H, 5.31; N, 4.39; F, 21.76. ^{1}H NMR (CD_3CN): OCH_2CH$_2$P, 3.92 ppm (dt, $^3J_{PH}$ = 18 Hz, $^3J_{HH}$ = 6 Hz); OCH$_2$CH_2P, 2.37 ppm (m); PCH_2CH$_3$, 2.10 ppm (m); uncoordinated CH_3CN, 1.96 ppm; PCH$_2$CH_3, 1.25 ppm (dt, $^3J_{PH}$ = 19 Hz, $^3J_{HH}$ = 8 Hz). IR (CH_2Cl_2): ν_{CN}, 2293 and 2321 cm^{-1}. A band observed at 2254 cm^{-1} is assigned to uncoordinated CH_3CN.

[Pd(POP)(CH_3CN)$_2$](BF_4)$_2$ (10b). This complex was pre-

pared in a manner analogous to that for $[Pd(POP\text{-}E)(CH_3CN)_2](BF_4)_2$ using bis((diphenylphosphino)ethyl)ether (POP) by mixing the solutions at −80 °C followed by warming to room temperature. ^1H NMR (acetone-d_6): Ph, 7.5−7.9 ppm (m); OCH_2CH_2P, 4.01 ppm (dt, $^3J_{PH}$ = 20 Hz, $^3J_{HH}$ = 6 Hz); OCH_2CH_2P, 3.23 ppm (m); CH_3CN, 1.95 ppm (s). IR (Nujol): ν_{CN}, 2298 and 2325 cm^{-1}.

$[Pd(POP\text{-}C)(CH_3CN)_2](BF_4)_2$ (10c). This complex was prepared in a manner analogous to $[Pd(POP\text{-}E)(CH_3CN)_2](BF_4)_2$ using bis((dicyclohexylphosphino)ethyl) ether (POP-C) as the ligand. The reaction conditions were 70 °C for 5 h. This complex could not be obtained analytically pure. On the basis of ^{31}P and ^1H NMR data, we estimate a purity of approximately 85%. The major phosphorus-containing impurity appears to be the trans complex in which oxygen is coordinated (see Table 2 for ^{31}P NMR data). ^1H NMR (acetone-d_6): PCH_2CH_2O, 4.19 ppm (dt, $^3J_{PH}$ = 16 Hz, $^3J_{HH}$ = 6 Hz); PCH_2CH_2O, C_6H_{11}, and CH_3CN, 1.2−2.8 ppm (m's). IR (CH_2Cl_2): ν_{CN}, 2294 and 2320 cm^{-1}.

$[Pd(POP)(PEt_3)](BF_4)_2$ (11b). Triethylphosphine (0.062 g, 0.52 mmol) was added via syringe to a solution of $[Pd(POP)(CH_3CN)_2](BF_4)_2$ (0.40 g, 0.50 mmol) in dichloromethane (30 mL). The reaction solution was stirred for 0.5 h, and then hexane was added to give a white precipitate. The product was recrystallized from a mixture of acetone and ether. The solid (0.32 g, 76%) was collected by filtration and dried in a vacuum. Anal. Calcd for $C_{34}H_{43}B_2F_8P_3PdO$: C, 48.58; H, 5.16; P, 11.05. Found: C, 48.10; H, 4.76; P, 10.62. ^1H NMR (CD_3CN): Ph, 7.6−8.0 ppm (m); OCH_2CH_2P, 4.01 ppm (m); OCH_2CH_2P, 3.16 ppm (q, splitting 4 Hz); PCH_2CH_3, 1.32 ppm (quintet, $^3J_{HH} = {}^2J_{PH}$ = 8 Hz); PCH_2CH_3, 0.79 ppm (dt, $^3J_{PH}$ = 19 Hz).

$[Pd(POP\text{-}E)(PEt_3)](BF_4)_2$ (11a). This compound was prepared according to the procedure described for $[Pd(POP)(PEt_3)](BF_4)_2$ using POP-E as the ligand. ^1H NMR (CD_3CN): OCH_2CH_2P, 4.14 ppm (m); OCH_2CH_2P, 2.48 ppm (m); PCH_2CH_3, 2.0, 2.1 ppm (m); PCH_2CH_3, 1.21, 1.19 ppm (overlapping triplets).

$[Pd(POP\text{-}C)(PEt_3)](BPh_4)_2{\cdot}NaBPh_4$ (11c). Triethylphosphine (0.2 mL) was added via syringe to a solution of $[Pd(POP\text{-}C)(CH_3CN)_2](BF_4)_2$ (1.0 mmol) prepared as described above. The reaction mixture was stirred for 1 h at room temperature, and then the solvent was removed on a vacuum line. The yellow solid that resulted was dissolved in acetonitrile (15 mL) and treated with a solution of $NaBPh_4$ (1.0 g) in ethanol (20 mL). The white microcrystalline precipitate that resulted was collected by filtration and dried in a vacuum (0.67 g, 40%). Anal. Calcd for $C_{106}H_{127}B_3NaP_3PdO$: C, 76.15; H, 7.66; Na, 1.38; P, 5.56. Found: C, 76.45; H, 7.18; Na, 1.18; P, 5.56. ^1H NMR (CD_3CN): Ph, 6.8−7.3 ppm (m); OCH_2CH_2P, 4.16 ppm (m); OCH_2CH_2P, C_6H_{11}, PCH_2CH_3, 1.3−2.5 (m's). The integration ratio expected for $Ph/OCH_2CH_2P/C_6H_{11}$, PCH_2CH_3, OCH_2CH_2P is 60/4/63, and the observed ratio is 60/4/66.

$[Pd(PSP)(CH_3CN)](BF_4)_2$ (7). A solution of bis((diphenylphosphino)ethyl) sulfide (PSP; 1.29 g, 2.82 mmol) in toluene (100 mL) was added to a solution of $[Pd(CH_3CN)_4](BF_4)_2$ (1.0 g, 2.3 mmol). The solution was stirred overnight, and then the solvent was removed with a vacuum line to yield an orange solid. This product was recrystallized from a mixture of acetonitrile and ether (0.75 g, 43%). Anal. Calcd for $C_{30}H_{31}B_2F_8NP_2PdS$: C, 46.22; H, 4.01; N, 1.80; P, 7.95. Found: C, 46.53; H, 4.11; N, 1.52; P, 7.90. ^1H NMR (acetone-d_6): Ph, 7.8−7.95, 7.6−7.8 ppm (m's); SCH_2CH_2P, 3.9−4.2 ppm (m); SCH_2CH_2P, 3.2−3.4 ppm (m); CH_3CN, 2.3 ppm (s). Addition of excess triethylphosphine to an NMR sample in CD_3CN resulted in the formation of $[Pd(PSP)(PEt_3)](BF_4)_2$. ^{31}P NMR data for this complex are given in Table 2.

$[Pd(PAsP)(CH_3CN)](BF_4)_2$ (8). A solution of PAsP (0.75 g, 1.18 mmol) in toluene (50 mL) was added to a solution of $[Pd(CH_3CN)_4](BF_4)_2$ (0.52 g, 1.2 mmol) in acetonitrile (75 mL). The reaction mixture was stirred for 2 h, and then the solvent was removed on a vacuum line. The yellow solid which resulted was recrystallized from a mixture of acetonitrile and ether (0.50 g, 50%). Anal. Calcd for $C_{36}H_{36}AsB_2F_8NP_2Pd$: C, 48.07; H, 4.03; N, 1.56; P, 6.89. Found: C, 47.94; H, 4.09; N, 1.57; P, 6.70. ^1H NMR (acetone-d_6): Ph, 7.35−7.95 ppm (m's); $AsCH_2CH_2P$, 3.0−3.9 ppm (m's); CH_3CN, 2.13 ppm (s). Addition of excess triethylphosphine to an NMR sample in CD_3CN resulted in the formation of $Pd(PAsP)(PEt_3)](BF_4)_2$. ^{31}P NMR data for this complex are given in Table 2.

Results

Synthesis of Ligands. With the exception of bis((diphenylphosphino)ethyl)phenylarsine (PAsP), the ligands used in this study were prepared by the reaction of the appropriate dihalide precursor with dialkyl or diaryl phosphide anions using slight modifications of literature methods.[11-17] PAsP was prepared by the base-catalyzed addition of diphenylphosphine to divinylphenylarsine. Free-radical catalyzed addition of diphenylphosphine to divinylphenylarsine does not occur, even though the analogous triphosphine ligand is readily prepared by this method. All the ligands are moderately air-sensitive in solution, especially those with terminal alkyl substituents. Spectroscopic data for all new ligands are given in the Experimental Section and Table 2. The data are fully consistent with the formation of linear PXP tridentate ligands.

Synthesis and Characterization of Metal Complexes. Reaction of 1,3-bis((diphenylphosphino)methyl)benzene (PCP) with $[Pd(CH_3CN)_4](BF_4)_2$ in a mixture of tetrahydrofuran and acetonitrile results in the formation of $[Pd(PCP)(CH_3CN)](BF_4)$ (**1**). This white complex is air stable in the solid state and in solution. A singlet at 43.2 ppm is observed in the ^{31}P NMR spectrum of **1**. This value is in the range expected for a diphenylphosphino group coordinated to palladium and part of a five-membered ring containing a Pd−C bond.[11] The triplet observed by ^1H NMR for the methylene protons (4.24 ppm, 4.9 Hz splitting, $^2J_{PH}$ = 9.8 Hz) confirms the presence of trans phosphorus ligands. A singlet at 2.24 ppm in acetone-d_6 is assigned to coordinated acetonitrile. Upon addition of acetonitrile, this resonance increases in height and shifts toward the position of free acetonitrile, which indicates a rapid exchange of acetonitrile for this complex. Two infrared bands at 2287 and 2316 cm^{-1} are also observed in dichloromethane. These bands are assigned to CN stretching and combination modes, respectively.[19] These spectroscopic data are consistent with a square-planar complex containing a metallated phenyl group trans to acetonitrile. Reaction of triethylphosphine with **1** results in the displacement of acetonitrile and the formation of $[Pd(PCP)(PEt_3)](BF_4)$ (**2**). This complex is also air stable in the solid state and in solution. The ^{31}P NMR spectrum consists of a doublet and a triplet assigned to the diphenylphosphino groups and coordinated triethylphosphine, respectively. The phosphorus−phosphorus coupling constant of 37 Hz indicates triethylphosphine coordinates cis to the diphenylphosphino groups, and the triplet observed for the methylene protons in the ^1H NMR spectrum confirms trans diphenylphosphino groups. This complex is also formulated as a square-planar complex in which the bridging phenyl group is metalated by palladium. An X-ray diffraction study of this complex confirms this assignment as discussed below.

(19) Storhoff, B. N.; Lewis, C. H., Jr. *Coord. Chem. Rev.* **1977**, *33*, 1.

Reaction of 2,6-((diphenylphosphino)methyl)pyridine, PNP, with $[Pd(CH_3CN)_4](BF_4)_2$ in acetonitrile results in a mixture of $[Pd(PNP)(CH_3CN)](BF_4)$ (**3**) and $\{[Pd(PNP)]_2(\mu\text{-PNP})\}(BF_4)_4$ (**4**), as shown in eq 1. The pres-

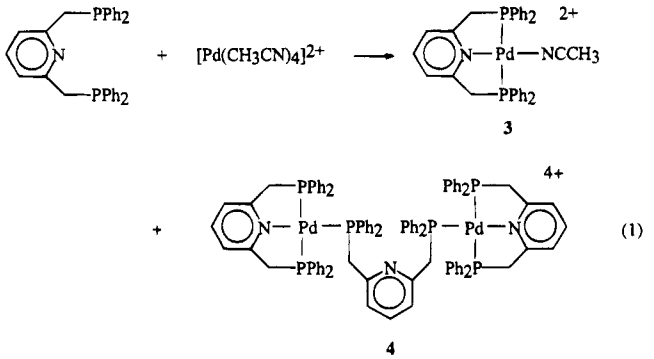

(1)

ence of **3** is indicated by a singlet at 38.0 ppm in the ^{31}P NMR spectrum consistent with a diphenylphosphino group in a five-membered ring.[20] A triplet resonance at 4.65 ppm in the ^1H NMR spectrum is assigned to the methylene protons bound to two trans phosphine ligands ($^2J_{PH}$ = 11.2 Hz, the splitting is 5.6 Hz). Dimer **4** exhibits a doublet at 41.4 ppm in the ^{31}P NMR spectrum assigned to the diphenylphosphino group of a chelating tridentate ligand and a triplet at 21.9 ppm ($^2J_{PP}$ = 18 Hz) assigned to the diphenylphosphino group of a bridging PNP ligand. The ^1H NMR spectrum contains a triplet at 4.75 ppm assigned to the methylene protons adjacent to the trans phosphorus atoms of **4** ($^2J_{PH}$ = 9.6 Hz, the splitting is 4.8 Hz) and a doublet at 2.78 ppm ($^2J_{PH}$ = 9.3 Hz) assigned to the methylene protons of the bridging PNP ligand. Repeated efforts to obtain **3** as a pure compound from various solvents were unsuccessful. However, addition of triethylphosphine to a reaction mixture of PNP and $[Pd(CH_3CN)_4](BF_4)_2$ produced $[Pd(PNP)(PEt_3)](BF_4)_2$ (**5**). This white complex is air stable in the solid state and in solution. The spectral data are similar to those of $[Pd(PCP)(PEt_3)](BF_4)$, and a structural determination confirms a square-planar structure with the triethylphosphine ligand trans to the pyridine nitrogen of the tridentate PNP ligand (see below).

As shown in eq 2, the reactions of the tridentate ligands containing the PNHP, PSP, and PAsP donor sets with $[Pd(CH_3CN)_4](BF_4)_2$ result in the formation of square-planar $[Pd(PXP)(CH_3CN)](BF_4)_2$ complexes. The

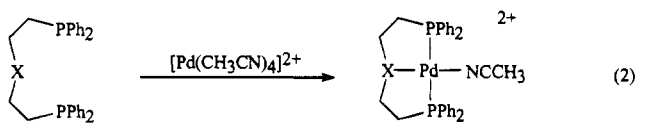

(2)

	X
6	NH
7	S
8	AsPh

spectroscopic data for **6** are typical of these complexes. The ^{31}P NMR spectrum consists of a singlet at 47.5 ppm in CD_3CN. This corresponds to a coordination chemical shift of 61 ppm (Table 2, column 4), which is similar to the value of 67 ppm observed for $[Pd(etp)(CH_3CN)](BF_4)_2$ (where etp is bis((diphenylphosphino)ethyl)phenylphosphine).[6] This result suggests that the phosphorus atoms are in five-membered rings and that the nitrogen atom of the tridentate ligand is coordinated to palladium. A resonance for the N*H* proton is observed at 6.9 ppm, which corresponds to a shift of 6 ppm from the free ligand in acetone-d_6. This shift is also consistent with coordination of nitrogen. The remaining coordination site of the square-planar complex is occupied by acetonitrile. A resonance for this ligand is observed at 2.61 ppm, which shifts upon addition of acetonitrile. The infrared spectrum shows a band at 2305 cm^{-1} assigned to the C–N stretching mode of coordinated acetonitrile. On the basis of similar spectroscopic data (see Experimental Section and Table 2), complexes **7** and **8** are assigned analogous structures. Complex **6** reacts with triethylphosphine to form $[Pd(PNHP)(PEt_3)](BF_4)_2$ (**9**). Spectral data for this complex are also consistent with a square-planar structure with nitrogen trans to triethylphosphine (see Experimental Section and Table 2).

The reaction of tridentate ligands containing the POP donor set with $[Pd(CH_3CN)_4](BF_4)_2$ results in the formation of complexes containing a chelating cis-diphosphine ligand in which the oxygen atom is not coordinated as shown in reaction 3. The remaining two coordination

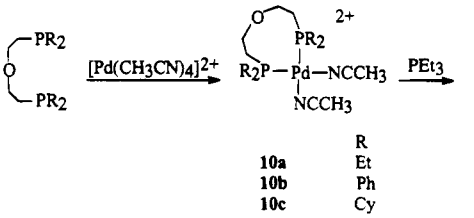

	R
10a	Et
10b	Ph
10c	Cy

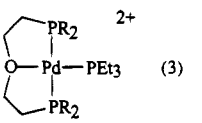

(3)

	R
11a	Et
11b	Ph
11c	Cy

sites are occupied by acetonitrile ligands. For complex **10b**, a single resonance is observed in the ^{31}P NMR spectrum at 19.8 ppm in CD_3CN. This corresponds to a coordination chemical shift of 35 ppm compared to a value of 61 ppm for $[Pd(PNHP)(CH_3CN)](BF_4)_2$ (**6**). The fact that the coordination chemical shift is 26 ppm smaller for **10b** than for **6** suggests that the oxygen may not be coordinated. The ring effect for a five-membered chelate ring is expected to be about 20 ppm.[20] The ^1H NMR data (acetone-d_6) are also consistent with this interpretation because the methylene protons adjacent to the oxygen atoms appear as a doublet of triplets at 4.01 ppm with a $^3J_{PH}$ coupling constant of 20 Hz and a $^3J_{HH}$ coupling of 6 Hz. A more complex multiplet, similar to the one observed for the NCH_2CH_2P protons of $[Pd(PNHP)(CH_3CN)](BF_4)_2$, is expected for this resonance if oxygen coordinates. The acetonitrile resonance at 1.95 ppm integrates for two CH_3CN ligands per molecule, consistent with the nitrogen analysis for this complex. An infrared spectrum exhibits bands at 2298 and 2325 cm^{-1} assigned to coordinated acetonitrile. The spectroscopic data obtained for $[Pd(POP\text{-}E)(CH_3CN)_2](BF_4)_2$ are similar to those for $[Pd(POP)(CH_3CN)_2](BF_4)_2$, and this complex is assigned the structure shown in eq

(20) Garron, P. E. *Chem. Rev.* **1981**, *81*, 229.

3 as well. ^1H and ^{31}P NMR spectra recorded on crude reaction mixtures obtained using POP-C as the ligand are consistent with the formation of a small amount, approximately 25%, of a trans complex, as well as a cis complex (see Experimental Section and Table 2). Complex **10c** could not be successfully purified for elemental analysis, however. Complex **10b** reacts with PEt_3 to form $[Pd(POP)(PEt_3)](BF_4)_2$ (**11b**). In this complex, the oxygen atom of the tridentate ligand is coordinated trans to triethylphosphine. The triethylphosphine resonance is a triplet and the diphenylphosphino resonance is a doublet. Coordination of the oxygen atom is indicated by the similarity of coordination chemical shift of 60 ppm for the diphenylphosphino resonance for $[Pd(POP)(PEt_3)](BF_4)_2$ compared to 61 ppm for $[Pd(PNHP)(PEt_3)](BF_4)_2$. The ^1H NMR resonance for the methylene group adjacent to oxygen is a complex multiplet and not a doublet of triplets as observed for **10b**. These data indicate that reaction of triethylphosphine with **10b** leads to a structural reorganization and formation of complex **11b** with a trans geometry. Spectral data for **11a** and **11c** support similar structural assignments.

Reactions with Acid and CO. Because the catalytic reduction of CO_2 by [Pd(triphosphine)(solvent)]$(BF_4)_2$ complexes requires the presence of acid, the effect of acid on complexes **1**−**11** was studied. $[Pd(PCP)(PEt_3)](BF_4)$ and $[Pd(PAsP)(PEt_3)](BF_4)_2$ react in 0.1 M HBF_4 acetonitrile solutions to form $[Pd(PCP)(CH_3CN)](BF_4)$ and $[Pd(PAsP)(CH_3CN)(BF_4)_2$, respectively, and protonated triethylphosphine. This behavior is similar to that observed previously for [Pd(triphosphine)(PR_3)]$(BF_4)_2$ complexes in acidic acetonitrile solutions.[6] In contrast, the triethylphosphine ligands of $[Pd(PNP)(PEt_3)](BF_4)_2$, $[Pd(PNHP)(PEt_3)](BF_4)_2$, $[Pd(PSP)(PEt_3)](BF_4)_2$, and $[Pd(POP\text{-}R)(PEt_3)](BF_4)_2$ are not protonated under these conditions. This difference in reactivity is attributed to the greater trans influence of C and As compared to N, S, and O. In dimethylformamide, the triethylphosphine ligand of $[Pd(PCP)(PEt_3)](BF_4)$ remains coordinated in the presence of HBF_4. Dimethylformamide solutions of $[Pd(PCP)(PEt_3)](BF_4)$ and $[Pd(PCP)(CH_3CN)](BF_4)$ are also unaffected by 0.1 M phosphoric acid. Therefore the catalytic waves observed for the latter complex in the presence of CO_2 and H_3PO_4 (see below) cannot be attributed to a phosphate derivative. Addition of HBF_4 to a mixture of $[Pd(PNP)(CH_3CN)](BF_4)_2$ and $\{[Pd(PNP)]_2\text{-}\mu\text{-}PNP\}(BF_4)_4$ in acetonitrile results in the disappearance of the dimer and the formation of $[Pd(PNP)(CH_3CN)](BF_4)_2$ (**3**), even though the triethylphosphine complex, $[Pd(PNP)(PEt_3)](BF_4)_2$, is not protonated under these conditions. As a result, the predominant species in solution is **3**. This permitted an evaluation of the catalytic activity of $[Pd(PNP)(CH_3CN)](BF_4)_2$ in acidic acetonitrile solutions even though this complex could not be isolated in pure form.

Because CO is the product of CO_2 reduction for [Pd(triphosphine)(solvent)]$(BF_4)_2$ complexes, the effect of CO on complexes **1**−**11** was investigated. $[Pd(PCP)(CH_3CN)](BF_4)$ reacts with CO in noncoordinating solvents, such as dimethylformamide or acetone, but not in acetonitrile. Addition of approximately one atmosphere of ^{13}CO to a dimethylformamide-d_6 solution of $[Pd(PCP)(CH_3CN)](BF_4)$ resulted in a broadening of the single ^{31}P resonance. At room temperature a broad resonance assigned to exchanging ^{13}CO is observed at 184 ppm in the ^{13}C NMR spectrum. At −30 °C, two resonances are observed at 185.2 ppm and 183.0 ppm which are assigned to free and coordinated CO, respectively. Infrared spectra obtained on 5×10^{-2} M dimethylformamide solutions of $[Pd(PCP)(CH_3CN)](BF_4)$ at 50 psi CO exhibited a single band at 1937 cm^{-1} assigned to coordinated CO. The binding of CO to $[Pd(PCP)(CH_3CN)](BF_4)$ is also supported by electrochemical studies (see below). All of these data support a rapid reversible binding of CO to $[Pd(PCP)(CH_3CN)](BF_4)$ as shown in reaction 4. When water and CO were added to a DMF

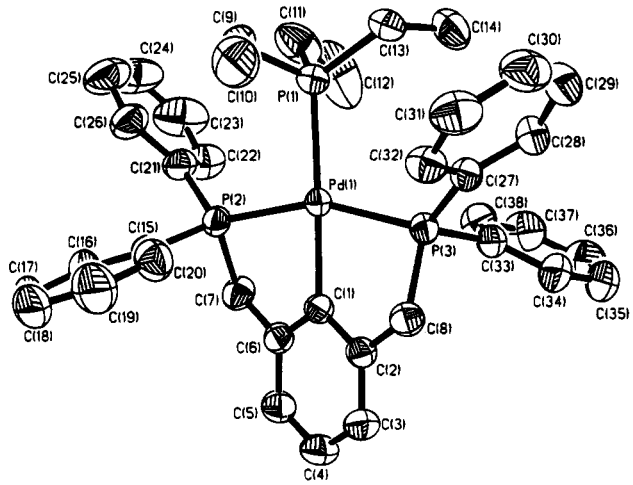

Figure 1. Drawing of the $[Pd(PCP)(PEt_3)]^+$ cation of **2** showing the atom-numbering scheme.

$$[Pd(PCP)(DMF)]^+ + CO \rightleftharpoons [Pd(PCP)(CO)]^+ + DMF \quad (4)$$

solution of $[Pd(PCP)(CH_3CN)](BF_4)$ in the presence of 2.5×10^{-2} M H_3PO_4, no H_2 was detected after several hours. This result indicates that $[Pd(PCP)(CH_3CN)](BF_4)$ is not a catalyst for the shift reaction under conditions where catalytic waves are observed by cyclic voltammetry. None of the other complexes shown in Table 2 react with CO, nor do the [Pd(triphosphine)$(CH_3CN)](BF_4)_2$ complexes prepared previously. For example, $[Pd(etpC)(CH_3CN)](BF_4)_2$ (where etpC is bis(dicyclohexylphosphinoethyl)phenylphosphine) does not react with CO at 400 psi in DMF as determined by IR spectroscopy.

Structural Studies. Crystals of $[Pd(PCP)(PEt_3)](BF_4)$ and $[Pd(PNP)(PEt_3)](BF_4)_2$ were most readily obtained from concentrated acetone solutions and consist of $[Pd(PCP)(PEt_3)]^+$ and $[Pd(PNP)(PEt_3)]^{2+}$ cations, respectively, and disordered BF_4 anions. Drawings of the two cations illustrating their basic structural features are shown in Figures 1 and 2. For $[Pd(PCP)(PEt_3)]^+$, the largest deviation of any atom from the plane defined by palladium, the three phosphorus atoms, and the metallated carbon atom is less than 0.02 Å. The coordination sphere of palladium in $[Pd(PNP)(PEt_3)]^{2+}$ is strictly planar as required by a twofold axis passing through the Pd−N and Pd−PEt_3 bonds. This twofold axis also requires that the PEt_3 ligand be disordered. Selected bond distances and angles for the two cations are shown in Table 3. The Pd−P (2.279−2.358 Å), Pd−C (2.075 Å), and Pd−N (2.107 Å) bond lengths are normal. The Pd−P bond lengths follow the order expected for a trans influence sequence of N < P < C. The P−Pd−C (79.0 and 79.1°) and P−Pd−N

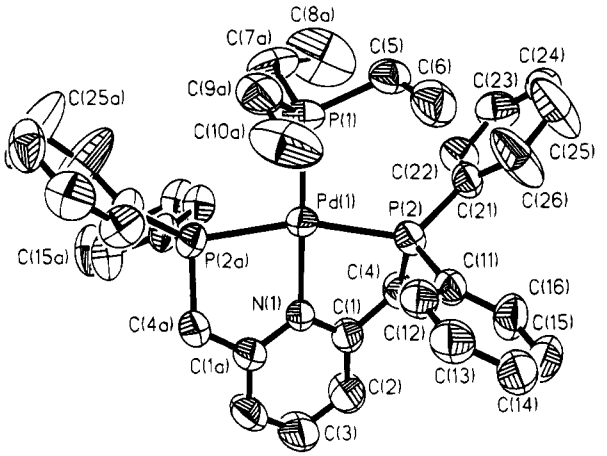

Figure 2. Drawing of the $[Pd(PNP)(PEt_3)]^{2+}$ cation of **5** showing the atom-numbering scheme.

Table 3. Selected Bond Lengths (Å) and Bond Angles (deg) for $[Pd(PCP)(PEt_3)](BF_4)$ and $[Pd(PNP)(PEt_3)](BF_4)_2$

$[Pd(PCP)(PEt_3)](BF_4)$		$[Pd(PNP)(PEt_3)](BF_4)_2$	
	Bond Lengths		
Pd(1)−P(1)	2.358(1)	Pd(1)−P(1)	2.279(2)
Pd(1)−C(1)	2.075(2)	Pd(1)−N(1)	2.107(4)
Pd(1)−P(2)	2.306(1)	Pd(1)−P(2)	2.319(1)
Pd(1)−P(3)	2.298(1)		
P(1)−C(9)	1.826(3)	P(1)−C(5)	1.913(9)
		P(1)−C(7A)	1.786(11)
P(2)−C(7)	1.824(2)	P(2)−C(4)	1.838(5)
P(3)−C(8)	1.834(3)		
C(2)−C(8)	1.498(3)	C(1)−C(4)	1.505(6)
C(6)−C(7)	1.503(4)		
C(1)−C(2)	1.400(3)	N(1)−C(1)	1.343(5)
C(2)−C(3)	1.392(3)	C(1)−C(2)	1.364(6)
C(3)−C(4)	1.382(4)	C(2)−C(3)	1.368(6)
	Bond Angles		
P(2)−Pd(1)−C(1)	79.0(1)	P(2)−Pd(1)−N(1)	80.3(1)
P(3)−Pd(1)−C(1)	79.1(1)		
P(1)−Pd(1)−P(2)	98.6(1)	P(1)−Pd(1)−P(2)	99.7(1)
P(1)−Pd(1)−P(3)	103.3(1)		
P(1)−Pd(1)−C(1)	177.7(1)	P(1)−Pd(1)−N(1)	180.0(1)
P(2)−Pd(1)−P(3)	158.1(1)	P(2)−Pd(1)−P(2A)	160.6(1)
Pd(1)−P(1)−C(9)	112.0(1)	Pd(1)−P(1)−(C5)	115.9(3)
		Pd(1)−P(1)−(C9A)	117.1(3)
Pd(1)−P(2)−C(7)	100.6(1)	Pd(1)−P(2)−C(4)	96.5(1)
Pd(1)−P(3)−C(8)	101.4(1)		
P(2)−C(7)−C(6)	104.8(2)	P(2)−C(4)−C(1)	108.4(3)
C(1)−C(6)−C(7)	118.1(2)	N(1)−C(1)−C(4)	116.8(4)
Pd(1)−C(1)−C(6)	120.2(2)	Pd(1)−N(1)−C(1)	120.2(2)
C(6)−C(1)−C(2)	118.8(2)	C(1)−N(1)−C(1A)	119.6(5)

(80.3°) angles formed between the phosphorus atoms and the carbon or nitrogen atoms of the tridentate ligands are significantly less than 90° and similar to the value of 80.8° reported for [Pd(PCP)Cl].[21] The P−Pd−P angles formed by the diphenylphosphino groups and triethylphosphine compensate by being much larger (98.6−103.3°). The small P−Pd−C and P−Pd−N angles of the tridentate ligand can be attributed to two ring effects. The P−Pd−P bond angles for the six-membered rings in $[Pd(dppp)X_2]$ (where dppp is 1,3-bis(diphenylphosphino)propane and X is NCS or Cl) and [Rh(ttp)Cl] (where ttp is bis((diphenylphosphino)ethyl)phenylphosphine) are 90 and 89.3 ± 0.7°, respectively.[22-24] Complexes with five-membered chelate rings have P−Pd−P angles of approximately 85°. For $[Pd(MesetpE)(CH_3CN)](BF_4)_2$ (where MesetpE is bis(diethylphosphinoethyl)mesitylphosphine), the P−Pd−P angle formed by the terminal and central phosphorus atoms of the triphosphine ligand is 87.5°.[25] The P−Pd−P angle for the five-membered rings in $[Pd(etp)]_2(BF_4)_2$ is 85.0°,[6] and for $[Pd(dppe)X_2]$ (where dppe is bis(diphenylphosphino)ethane and X is NCS or Cl) the P−Pd−P angles are approximately 85°.[22,23] $\{Pd[^tBu_2P(CH_2)_2CH(CH_2)_2P^tBu_2](CH_3)\}$ and $\{Pd[^tBu_2P(CH_2)_2CH(CH_2)_2P^tBu_2](OH_2)\}(BPh_4)$ have slightly smaller angles of 83−84°.[26] This small decrease for the latter two complexes is attributed to the shorter Pd−C bonds compared to Pd−P bonds. The Pd−P and Pd−C bond lengths for the latter two complexes are very similar to the Pd−P, Pd−C, and Pd−N bond lengths of $[Pd(PCP)(PEt_3)](BF_4)$ and $[Pd(PNP)(PEt_3)](BF_4)_2$. Incorporation of the phenyl and pyridine rings into the backbones of the tridentate ligands appears to result in further reductions of the P−Pd−C and P−Pd−N angles by 3−4°. The net result is an approximately 5° reduction in the chelate angle when phenyl or pyridine rings are substituted for phosphorus in tridentate ligands containing two carbon backbones. This is comparable to the difference observed between five- and six-membered chelate rings for tridentate ligands with all phosphorus donor atoms.

Electrochemical Studies. The electrochemical data for all of the complexes described above are summarized in Table 4. A plot of i_p of the first cathodic wave vs the square root of the scan rate is linear for the ranges shown in column 6 indicating all the complexes undergo diffusion-controlled reductions.[27] For the triethylphosphine complexes, the waves correspond to two-electron processes. The cyclic voltammogram of $[Pd(PNP)(PEt_3)](BF_4)_2$ is shown in Figure 3(a). For this complex, a single reversible two-electron reduction wave is observed. The difference between the peak potentials for the cathodic and anodic waves, ΔE_p, is 38 mV at a sweep rate of 20 mV/s. This value is less than the 60 mV value required for a one-electron process and consistent with a two-electron process for which a value of 30 mV is expected.[28] A second criterion for determining the number of electrons involved in the cathodic waves is the difference between the peak potential and the potential at half-height, $E_p - E_{p/2}$. $E_p - E_{p/2}$ should be 28 mV for a two-electron process and 57 mV for a one-electron process.[27] The 27 mV value observed for $[Pd(PNP)(PEt_3)](BF_4)_2$ at 20 mV/s implies a two-electron reduction. The other triethylphosphine complexes listed in Table 4 have $E_p - E_{p/2}$ values ranging from 37 to 50 mV at 50 mV/s, with the exception of $[Pd(PAsP)(PEt_3)](BF_4)_2$. These values are less than the 57 mV required for one-electron processes and are more consistent with a two-electron reduction slightly broadened by slow electron-transfer processes or uncompensated resistance. With the exception of $[Pd(PNP)(PEt_3)](BF_4)_2$, controlled-potential electrolyses of the triethylphosphine

(21) Gorla, F.; Venanzi, L. M.; Albinati, A. *Organometallics* **1994**, *13*, 43.
(22) Palenik, G. J.; Matthew, M.; Steffen, W. L.; Beran, G. *J. Am. Chem. Soc.* **1975**, *97*, 1059.
(23) Steffen, W. L.; Palenik, G. J. *Inorg. Chem.* **1976**, *15*, 2432.
(24) Nappier, T. E.; Meek, D. W.; Kirchner, R. M.; Ibers, J. A. *J. Am. Chem. Soc.* **1973**, *95*, 4194.
(25) Bernatis, P. R.; Miedaner, A.; Haltiwanger, R. C.; DuBois, D. L. *Organometallics*, preceding article in this issue.
(26) Seligson, A. L.; Trogler, W. C. *Organometallics* **1993**, *12*, 738.
(27) Andrieux, C. P.; Savéant, J. M. In *Investigation of Rates and Mechanisms of Reactions*; Bernasconi, C. F., Ed.; Wiley: New York, 1986; Vol. 6, 41E, Part 2, 305.
(28) Bard, A. J.; Faulkner, L. R. *Electrochemical Methods*; Wiley: New York, 1980; 229.

Table 4. Electrochemical Data for Palladium Complexes Containing Tridentate Ligands in Dimethylformamide

compound	$E_p/E_{1/2}$[a]	ΔE_p ($E_p - E_{p/2}$)[b]	i_p (μA)[c]	n[d]	range[e]
[Pd(PCP)(CH_3CN)](BF_4), **1**	−1.99 i	(62)	0.76	1.09	50−1000
[Pd(PCP)(PEt_3)](BF_4), **2**	−2.20 i	(45)	1.78	2.25	50−1000
[Pd(PNP)(CH_3CN)](BF_4)$_2$, **3**[g]	−1.04 i	(47)			
{[Pd(PNP)]$_2$-μ-PNP}$_2$(BF_4)$_4$, **4**[g]	−1.28 i				
	−1.57 i[f]				
[Pd(PNP)(PEt_3)](BF_4)$_2$, **5**	−1.22 r	46 (31)	1.92	1.48	20−400
[Pd(PNHP)(CH_3CN)](BF_4)$_2$, **6**	−1.05 i	(62)	0.72	0.94	50−1000
	−1.58 i[f]				
[Pd(PNHP)(PEt_3)](BF_4)$_2$, **9**	−1.30 q	143 (37)	1.84	1.89	50−1000
	−1.36 i[f]				
[Pd(PSP)(CH_3CN)](BF_4)$_2$, **7**	−0.91 i	(42)	1.00	0.76	50−2000
	−1.43 i[f]				
[Pd(PSP)(PEt_3)](BF_4)$_2$	−1.03 r	43 (35)	2.66		
[Pd(PAsP)(CH_3CN)](BF_4)$_2$, **8**	−1.10 i	(78)	1.34	1.01	50−400
Pd(PAsP)(PEt_3)](BF_4)$_2$	−1.05 q	165 (79)	1.78		
[Pd(POP-E)(CH_3CN)$_2$](BF_4)$_2$, **10a**	−1.44 i	(96)	0.86	1.29	50−4000
[Pd(POP-E)(PEt_3)](BF_4)$_2$, **11a**	−1.08 r	(50)	2.04	1.98	50−4000
[Pd(POP)(CH_3CN)$_2$](BF_4)$_2$, **10b**	−0.91 i	(63)	0.70	1.6	50−400
	−0.97 i				
[Pd(POP)(PEt_3)](BF_4)$_2$, **11b**	−0.88 r	(41)	1.74	1.92	20−400
	−0.73 q	(98)			
[Pd(POP-C)(CH_3CN)$_2$](BF_4)$_2$, **10c**	−1.01 i	(86)	0.72	0.99	50−4000
[Pd(POP-C)(PEt_3)](BPh_4)$_2$, **11c**	−1.02 i	43 (35)	1.99	1.85	50−4000

[a] Peak potentials, E_p, versus the ferrocene/ferrocenium couple for irreversible waves or half-wave potentials, $E_{1/2}$, for reversible or quasi-reversible waves. The letters i, r, and q designate whether the wave appears irreversible (no anodic wave), reversible, or quasi-reversible. [b] Peak-to-peak separation (ΔE_p) or the difference in the peak potential and the potential at half height ($E_p - E_{p/2}$). All values are for a scan rate of 50 mV/s. [c] Current observed for complexes at glassy carbon electrodes (1-mm diameter) for 1.0×10^{-3} M solutions of each respective complex. [d] Number of faradays passed/mol of complex during controlled-potential electrolysis experiments. [e] Range of scan rates in mV/s for which plots of i vs. $v^{1/2}$ are linear. [f] This cathodic wave is assigned to a palladium(I) dimer for reasons discussed in text for [Pd(PNHP)(CH_3CN)](BF_4)$_2$. [g] Electrochemical experiments carried out in acetonitrile.

complexes carried out at potentials 100 mV negative of the peak potential results in the passage of 2.0 ± 0.2 faradays/mol of complex. These values support two-electron processes for these complexes. The rather low value of 1.48 faradays/mol observed for [Pd(PNP)(PEt_3)](BF_4)$_2$ is attributed to reaction of a Pd(0) intermediate with a Pd(II) species in solution. Although this reaction is slow on the cyclic voltammetry time scale, it becomes significant in the time required for the bulk electrolysis experiments (approximately 0.5 h). Both cyclic voltammograms and ^{31}P NMR spectra recorded on reduced solutions of [Pd(PNP)(PEt_3)](BF_4)$_2$ indicate the presence of multiple products.

Although the cathodic waves for the triethylphosphine complexes are assigned to two-electron reductions with relatively fast electron-transfer kinetics, the reoxidation of the reduced species is quite variable. For the [Pd(PNP)(PEt_3)](BF_4)$_2$ complex shown in Figure 3a, the reoxidation is facile at low scan rates with a ΔE_p of 38 mV and i_{pc}/i_{pa} ratio of 0.89 at 10 mV/s scan rate. At a scan rate of 4 V/s, these values are 70 mV and 0.43, respectively. These results are consistent with a slow rearrangement of the reduced species to a configuration appropriate for reoxidation. A similar behavior is observed for [Pd(PNHP)(PEt_3)](BF_4)$_2$ for which the reoxidation is slow even at relatively slow scan rates; i.e., ΔE_p is 143 mV at 50 mV/s.

The cyclic voltammogram of [Pd(POP)(PEt_3)](BF_4)$_2$ is shown in Figure 3b. This complex exhibits two anodic waves at a 50 mV/s scan rate. As the scan rate increases, the second anodic wave, a_2, decreases until at 1 V/s this wave is no longer observed. In this case, the ratio of the currents i_{a1}/i_{c1} increases from 0.71 at 20 mV/s to 0.97 at 4 V/s. These results are consistent with an isomerization of the complex following reduction to form a new species observed at a_2. Cyclic voltammograms recorded on solutions reduced by 2 faradays/mol of complex exhibit a large quasi-reversible wave at −0.73 V that corresponds to a new cathodic peak c_2 and the anodic peak a_2. The wave observed at −0.88 V, a_1 and c_1, is much smaller and accounts for approximately 30% of the reduced species. This result is consistent with the formation of two palladium(0) complexes. These two complexes are also observed by ^{31}P NMR spectroscopy. The analogous [Pd(POP-E)(PEt_3)](BF_4)$_2$ complex exhibits a single reversible two-electron wave at −1.08 V with no reaction following reduction.

For the complex [Pd(PCP)(PEt_3)](BF_4), the peak potential of the cathodic wave shifts to more negative potentials by 19 mV upon changing the scan rate from 100 mV/s to 1 V/s. A value of 15 mV is expected for reversible two-electron reduction followed by a fast irreversible chemical reaction. This irreversible reaction leads to products that have three very small anodic waves at −0.46, −0.65, and −0.86 V. The species responsible for these waves have not been identified.

The peak currents of the acetonitrile complexes are significantly smaller than for the triethylphosphine complexes (Table 4, column i_p). The ratio of the peak current for a reversible two-electron reduction to the peak current for a reversible one-electron reduction, which is followed by a fast irreversible reaction, is expected to be 2.55 if the complexes have the same diffusion coefficients.[27] Because all of the complexes are roughly the same size and shape, their diffusion coefficients should be similar. The ratios of the peak current for each triethylphosphine complex to the analogous acetonitrile complex range from 2.56 for [Pd(PNHP)(PEt_3)](BF_4)$_2$/[Pd(PNHP)(CH_3CN)](BF_4)$_2$ to 2.34 for [Pd(PCP)(PEt_3)](BF_4)/[Pd(PCP)(CH_3CN)](BF_4). These values are fully consistent with two-electron reduction waves for the triethylphosphine complexes and one-electron reduction waves for the acetonitrile complexes.

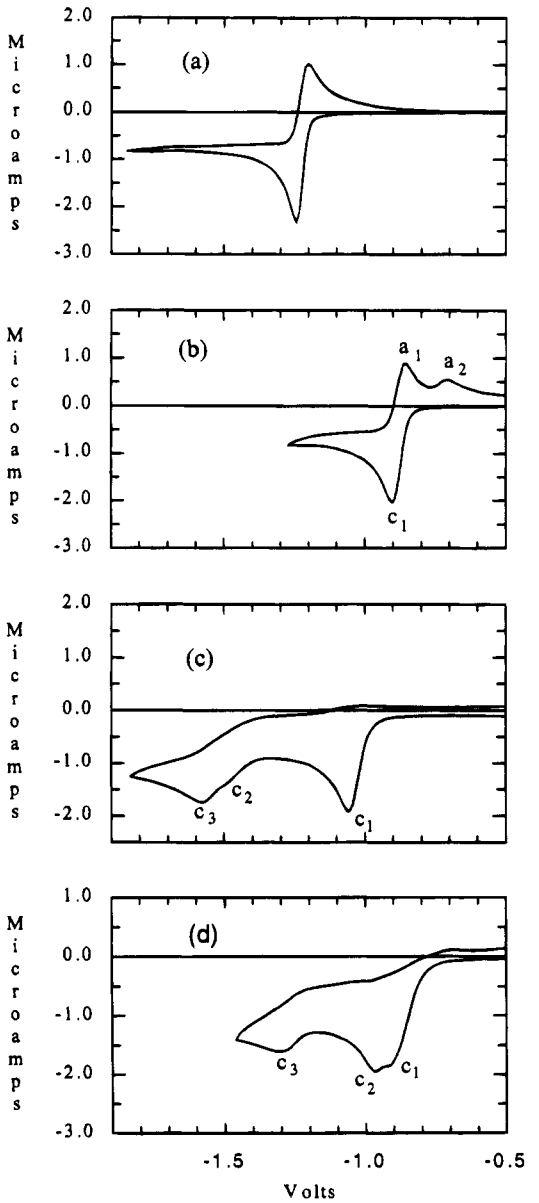

Figure 3. (a) Cyclic voltammogram of 1.6×10^{-3} M [Pd(PNP)(PEt$_3$)](BF$_4$)$_2$ (**5**) (20 mV/s). (b) Cyclic voltammogram of 1.8×10^{-3} M [Pd(POP)(PEt$_3$)](BF$_4$)$_2$ (**11b**) (20 mV/s). (c) Cyclic voltammogram of 1.8×10^{-3} M [Pd(PNHP)(CH$_3$CN)](BF$_4$)$_2$ (**6**) (50 mV/s). (d) Cyclic voltammogram of 2.4×10^{-3} M [Pd(POP)(CH$_3$CN)$_2$](BF$_4$)$_2$ (**10b**) (50 mV/s). The solutions were 0.3 M NEtBF$_4$ in dimethylformamide, and the working electrode was glassy carbon.

For the acetonitrile complexes the first cathodic waves correspond to reversible one-electron reductions followed by irreversible chemical reactions. The cyclic voltammogram of [Pd(PNHP)(CH$_3$CN)](BF$_4$)$_2$ is shown in Figure 3c. It consists of one large cathodic wave at −1.05 V, c_1, and two smaller cathodic waves at −1.49 and −1.58 V, c_2 and c_3, respectively. The difference in the peak potential and the potential at half-height, $E_p - E_{p/2}$, for c_1 is 62 mV. This is somewhat larger than the 48 mV value expected for a one-electron E_rC_i process. However, the ratio of the currents for the first cathodic waves of [Pd(PNHP)(PEt$_3$)](BF$_4$)$_2$ and [Pd(PNHP)(CH$_3$CN)](BF$_4$)$_2$ indicates the former undergoes a two-electron reduction whereas the latter undergoes a one-electron reduction. The peak potential of c_1 shifts to more negative potentials by 30 mV on changing the scan rate from 100 to 1000 mV/s. This 30 mV shift in potential is consistent with a one-electron E_rC_i scheme.[27] The two smaller waves at −1.49 and −1.58 V decrease in magnitude relative to the first wave as the scan rate increases. This suggests that these two waves arise from chemical reactions following the initial one-electron reduction. The wave c_3 increases in relative magnitude as the concentration increases. Exhaustive reduction of [Pd(PNHP)(CH$_3$CN)](BF$_4$)$_2$ at −1.15 V resulted in the passage of 0.94 faradays/mol of complex consistent with a one-electron reduction. The product of this reduction was characterized by ^{31}P NMR spectroscopy (two doublets at 19.6 and 25.4 ppm, J = 10 Hz), UV−visible spectroscopy (λ_{max} = 434 nm), and cyclic voltammetry (irreversible cathodic wave at −1.58 V and an irreversible anodic wave at +0.40 V). These spectral and electrochemical data are very similar to data previously reported for the structurally characterized [Pd(triphosphine)]$_2$(BF$_4$)$_2$ dimers.[6] On this basis, wave c_3 in Figure 3c is attributed to the Pd(I) dimer [Pd(PNHP)]$_2$(BF$_4$)$_2$. The complexes [Pd(PCP)(CH$_3$CN)](BF$_4$)$_2$, [Pd(PSP)(CH$_3$CN)](BF$_4$)$_2$, and [Pd(PAsP)(CH$_3$CN)](BF$_4$)$_2$ exhibit one cathodic wave each in the range +1.0 to −2.0 V. The peak currents and $E_p - E_{p/2}$ values (Table 4) and peak potential shifts as a function of scan rate are similar to those observed for [Pd(PNHP)(CH$_3$CN)](BF$_4$)$_2$. Therefore the cathodic waves observed for [Pd(PCP)(CH$_3$CN)](BF$_4$), [Pd(PSP)(CH$_3$CN)](BF$_4$)$_2$, and [Pd(PAsP)(CH$_3$CN)](BF$_4$)$_2$ are also assigned to one-electron reductions followed by fast irreversible chemical reactions.

The cyclic voltammogram for [Pd(POP)(CH$_3$CN)$_2$](BF$_4$)$_2$ is shown in Figure 3d. It consists of cathodic waves at −0.91, −0.97, and −1.30 V. Chronocoulometric experiments were carried out in which the potential was stepped from −0.6 V to −1.1 V for [Pd(POP)(CH$_3$CN)$_2$](BF$_4$)$_2$ and [Pd(POP)(PEt$_3$)](BF$_4$)$_2$. As discussed above, the latter complex undergoes a two-electron reduction. The ratio of the slopes observed for the chronocoulometric plots of these two complexes was 0.83. This result is consistent with the waves at −0.91 and −0.97 V corresponding to two successive one-electron reductions. A controlled-potential electrolysis experiment carried out at −1.1 V resulted in the passage of 1.6 faradays/mol of complex and a variety of products as indicated by cyclic voltammograms and ^{31}P NMR spectra recorded on the reduced solutions. The electrochemical behaviors of [Pd(POP-E)(CH$_3$CN)$_2$](BF$_4$)$_2$ and [Pd(POP-C)(CH$_3$CN)](BF$_4$)$_2$ are similar to that of [Pd(POP)(CH$_3$CN)$_2$](BF$_4$)$_2$, and relevant data are given in Table 4.

Catalytic Studies. Figure 4 shows a cyclic voltammogram of [Pd(PCP)(CH$_3$CN)](BF$_4$) in a dimethylformamide solution under a N$_2$ atmosphere (solid line). The dotted line in Figure 4 is of the same solution saturated with CO$_2$ (0.18 M at 620 mmHg). The positive shift of the wave in the presence of CO$_2$ indicates a reaction with the Pd(I) intermediate generated upon reduction. The reaction of this intermediate with CO$_2$ must be faster or comparable in rate to the irreversible reaction occurring in the absence of CO$_2$, otherwise CO$_2$ would not produce a shift in the peak potential. Figure 5 shows the cyclic voltammograms of [Pd(PCP)(CH$_3$CN)](BF$_4$) in 0.015 M H$_3$PO$_4$ solutions purged with nitrogen (solid line) and purged with CO$_2$ (dotted line). A sig-

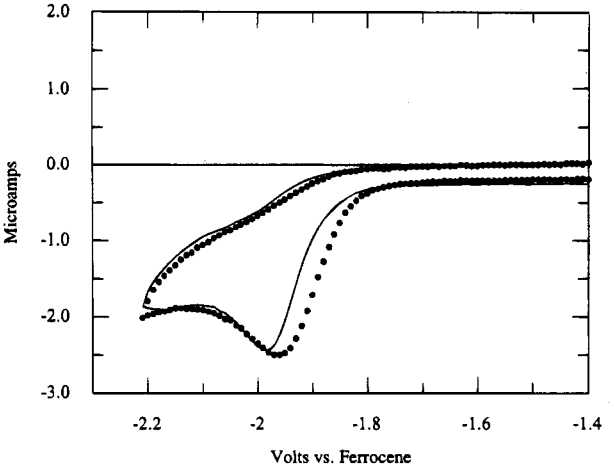

Figure 4. (a) Cyclic voltammogram of 2.1×10^{-3} M [Pd(PCP)(CH_3CN)](BF_4) (**1**) under nitrogen (solid line). (b) Same solution saturated with CO_2 at a pressure of 620 mm Hg (dotted line). Both scans were recorded at 100 mV/s.

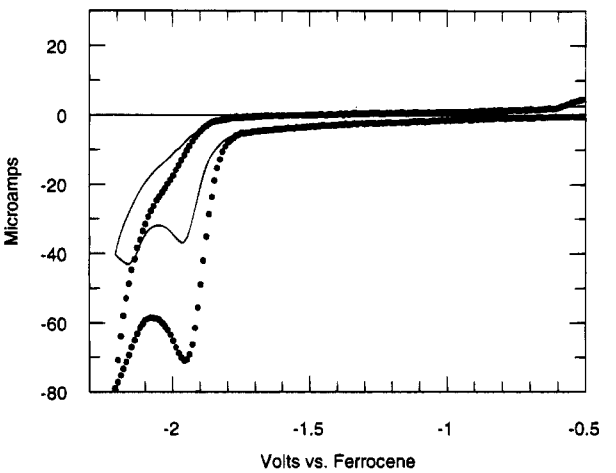

Figure 5. (a) Cyclic voltammogram of 2.1×10^{-3} M [Pd(PCP)(CH_3CN)](BF_4) (**1**) under nitrogen in the presence of 1.5×10^{-2} M H_3PO_4 (solid line). (b) Same solution saturated with CO_2 at 620 mm Hg (dotted line). The scan rate was 100 mV/s.

nificant increase in the current is observed in the presence of CO_2 compared to N_2. It is tempting to attribute the increased current in the presence of CO_2 to electrochemical reduction of CO_2. However, controlled-potential electrolysis experiments carried out on solutions containing 1×10^{-3} M [Pd(PCP)(CH_3CN)](BF_4), 0.03 M H_3PO_4, and 0.18 M CO_2 using reticulated vitreous carbon at −2.05 V resulted in the production of H_2 with a current efficiency of 100% as determined by gas chromatography. For this catalyst the turnover number is low, and only 4 or 5 mol of hydrogen are produced per mole of catalyst before the catalytic current decays to less than 10% of its original value.

The dependence of the current on CO_2 and acid concentrations is shown in Figure 6 for solutions of [Pd(PCP)(CH_3CN)](BF_4) in dimethylformamide. For a reversible electron-transfer reaction followed by a fast catalytic reaction, the current is given by eq 5.[29,30] In

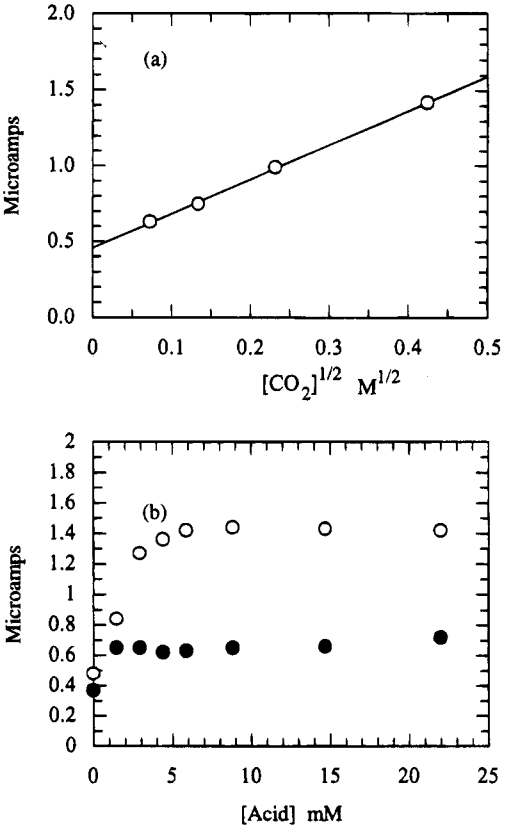

Figure 6. (a) Plot of the catalytic current versus $[CO_2]^{1/2}$ for a DMF solution of [Pd(PCP)(CH_3CN)](BF_4) (**1**) (5.4×10^{-4} M) and H_3PO_4 (0.03 M). (b) Plot of the current observed by cyclic voltammetry for a DMF solution of [Pd(PCP)(CH_3CN)](BF_4) (5.4×10^{-4} M) as a function of H_3PO_4 concentration. The solid circles represent the current in the presence of nitrogen. The open circles show the current in the presence of CO_2 (0.18 M). The scan rates were 20 mV/s.

$$\frac{i_c}{i_d} = \frac{\sigma}{0.447}\sqrt{\frac{RT}{nF}}\sqrt{\frac{kC_z^{\,m}}{v}} \qquad (5)$$

eq 5, i_c is the catalytic current, i_d is the peak current due to reversible reduction of the catalyst, σ is a factor which depends on the mechanism, n is the number of electrons transferred to the catalyst from the electrode, F is the Faraday constant, k is the rate constant for the reaction, C_z is the substrate concentration, v is the scan rate, and m is the order of the substrate in the rate-determining reaction. The derivation of this equation assumes that the concentrations of the substrates, C_z, are large compared to the concentration of the catalyst so that pseudo-first-order kinetics apply. From this equation it can be seen that current should exhibit an $m/2$ dependence on the substrate concentration. The square-root dependence of the current on CO_2 concentration observed in Figure 6a implies that the rate-determining step in hydrogen production is first order in CO_2 at the given acid concentration. As seen in Figure 6b, the catalytic current first increases linearly with acid concentration and then becomes independent of it. This is consistent with a change in the rate-determining reaction on going from low to high acid concentrations. The linear dependence at low acid concentrations is consistent with the rate-determining step being second order in acid under these conditions, but the concentration range is too small for an unam-

(29) Hammouche, M.; Lexa, D.; Momenteaux, M.; Savéant, J. M. *J. Am. Chem. Soc.* **1991**, *113*, 8455.
(30) Savéant, J. M.; Vianello, E. *Electrochim. Acta* **1965**, *10*, 905. Savéant, J. M.; Su, K. B. *J. Electroanal. Chem.* **1985**, *196*, 1. Nadjo, L.; Savéant, J. M.; Su, K. B. *Ibid.*, 23.

biguous determination of the reaction order. The independence of the current on acid concentrations above 5 $\times 10^{-3}$ M implies that acid does not play a role in the rate-determining step at these higher acid concentrations. A similar dependence of catalytic current on acid and CO_2 concentrations was observed previously for [Pd(triphosphine)(CH_3CN)](BF_4)$_2$ complexes. For these catalysts, however, CO is the main reduction product.[6,25] These results suggest that the rate-determining step at high acid concentrations is the same even though different products are formed.

For an ideal catalytic reaction, the current should be independent of the sweep rate[29] as shown by eq 5. However, [Pd(PCP)(CH_3CN)](BF_4) does not exhibit this ideal behavior; instead, the ratio of catalytic current to diffusion current has a constant value of 2.6. Rate constants calculated from cyclic voltammograms using eq 5 and a stoichiometric factor of 2 exhibit a linear dependence on the scan rate from 20 mV/s to 20 V/s. The lower currents observed at slower scan rates are attributed to rapid deactivation of the catalyst. This is consistent with the low turnover number of 4–5 observed for hydrogen production.

Catalytic waves are also observed for [Pd(PAsP)(CH_3CN)](BF_4)$_2$ and [Pd(PSP)(CH_3CN)](BF_4)$_2$ in dimethylformamide solutions. The increase in current observed for [Pd(PAsP)(CH_3CN)](BF_4)$_2$ in the presence of CO_2 and 0.1 M HBF_4 is comparable to that observed for [Pd(PCP)(CH_3CN)](BF_4), whereas that for [Pd(PSP)(CH_3CN)](BF_4)$_2$ is much smaller. For both [Pd(PAsP)(CH_3CN)](BF_4)$_2$ and [Pd(PSP)(CH_3CN)](BF_4)$_2$, the only product observed during bulk electrolysis is hydrogen, but for these complexes the turnover numbers are one or less. Detection of CO for such low turnovers was not possible. The complexes [Pd(POP)(CH_3CN)$_2$](BF_4)$_2$ and [Pd(POP-E)(CH_3CN)$_2$](BF_4)$_2$ do not exhibit catalytic currents in the presence of CO_2 and acid for the first reduction wave of these complexes. However, small catalytic currents are observed at potentials approximately one volt negative of the first cathodic wave in acidic acetonitrile solutions. These waves appear to arise from unstable intermediates because experiments carried out on reduced solutions of the complexes in the presence of CO_2 and acid failed to exhibit catalytic currents. Because the catalytic currents are small and appear to arise from unstable intermediates with undesirably negative potentials, the observed catalytic activity was not pursued further. We have previously observed that [Pd(diphos)(CH_3CN)$_2$](BF_4) complexes are not catalysts for CO_2 reduction,[31] and the results described here for the first cathodic wave of [Pd(POP-R)(CH_3CN)$_2$](BF_4)$_2$ are consistent with that observation.

Discussion

Synthesis. Reactions of tridentate ligands containing PCP, PNP, PNHP, PSP, and PAsP donor sets with [Pd(CH_3CN)$_4$](BF_4)$_2$ result in the formation of square-planar complexes with the C, N, S, or As atoms of the tridentate ligand trans to acetonitrile. In contrast, the POP-R ligands form square-planar complexes in which the oxygen atoms are not coordinated and the phosphorus atoms are cis. The remaining two sites are occupied by acetonitrile. Apparently, the weak Pd–O bonds are not sufficiently strong to force two phosphorus atoms into trans positions as observed for the other complexes. All of the acetonitrile complexes, including those with POP-R ligands, react with triethylphosphine to form square-planar complexes with triethylphosphine trans to the central donor atom of the tridentate ligands. For [Pd(PCP)(PEt_3)](BF_4) and [Pd(PNP)(PEt_3)](BF_4)$_2$, this basic structural arrangement has been verified by X-ray diffraction studies. Replacement of an acetonitrile ligand in [Pd(POP-R)(CH_3CN)$_2$](BF_4)$_2$ with PEt_3 results in a complex in which two of the phosphorus atoms must be in trans positions regardless of whether the oxygen atom coordinates. Coordination of the oxygen atom results in an energetically favorable situation in which a ligand with a very weak trans influence is trans to phosphorus, which has a strong trans influence. Previous structural studies of [Ni(POP)X_2][32] and [Rh(POP)(CO)](PF_6)[33] have also demonstrated that POP ligands can function as either bidentate or tridentate ligands, respectively.

NMR Studies. The chemical shifts of the triethylphosphine resonances for the complexes shown in Table 2 span a range of 60 ppm. The most positive chemical shift values are observed for complexes of the POP-R ligands, whereas [Pd(ttp)(PEt_3)](BF_4)$_2$ (where ttp is bis((diphenylphosphino)propyl)phenylphosphine)[34] has the most negative chemical shift. Large positive chemical-shift values have been associated previously with a small trans influence.[35] Using this criterion, the trans-influence order of the tridentate ligands shown in Table 2 is as follows: ttp > PCP > etp > PAsP > PNP ≅ PNHP > PSP > POP-R. This order is consistent with the observation that the coordinated triethylphosphine ligand reacts with acid to form $HPEt_3^+$ in acetonitrile solutions for the PCP, triphosphine, and PAsP complexes, but no protonation of triethylphosphine is observed for the PNP, PNHP, PSP, or POP-R complexes. For [Pd(ttp)(PEt_3)](BF_4)$_2$, coordination of triethylphosphine is not observed even in neutral acetonitrile solutions.[34] Less strongly coordinating solvents, such as acetone or dichloromethane, are required before triethylphosphine coordination is observed.

Electrochemical Studies. The acetonitrile complexes listed in Table 4 undergo reversible or quasi-reversible one-electron reductions followed by fast irreversible chemical reactions. Similar behavior was observed previously for the [Pd(triphosphine)(CH_3CN)](BF_4)$_2$ complexes, which undergo two closely-spaced one-electron reductions followed by irreversible chemical reactions.[6,25] For the latter complexes, catalytic activity can easily be detected by cyclic voltammetry.[6,25] Of the complexes shown in Table 4, only [Pd(PCP)(CH_3CN)](BF_4), [Pd(PAsP)(CH_3CN)](BF_4)$_2$, and [Pd(PSP)(CH_3CN)](BF_4)$_2$ exhibit catalytic currents arising from interaction with CO_2. For these complexes, hydrogen is the observed reduction product, and turnover numbers are low. Substitution of the central phosphorus atom

(31) Miedaner, A.; Haltiwanger, R. C.; DuBois, D. L. *Inorg. Chem.* **1991**, *30*, 417.

(32) Dapporto, P.; Sacconi, L. *J. Am. Chem. Soc.* **1970**, *92*, 4133. Dahlhoff, W. V.; Nelson, S. M. *J. Chem. Soc. A* **1971**, 2184. Greene, P. T.; Sacconi, L. *J. Chem. Soc. A* **1970**, 866.

(33) Alcock, N. W.; Brown, J. M.; Jeffery, J. C. *J. Chem. Soc., Dalton Trans.* **1976**, 583.

(34) Miedaner, A.; DuBois, D. L. Unpublished results.

(35) Hohman, W. H.; Kountz, D. J.; Meek, D. W. *Inorg. Chem.* **1986**, *25*, 616.

of the tridentate ligand with C, N, O, As, and S is detrimental with respect to CO_2 reduction.

For [Pd(PCP)(CH_3CN)](BF_4), the biphasic dependence of the catalytic current on acid concentration (Figure 6b) is consistent with two different rate-determining steps in the catalytic cycle. The square-root dependence of the catalytic current on CO_2 concentration at high H_3PO_4 concentrations (Figure 6a) indicates the rate-determining step under these conditions is a first-order reaction of CO_2 with a Pd(I) intermediate. An intermediate such as **12** would readily account for the

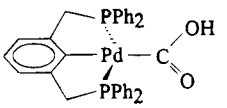

12

observed CO_2 dependence, and there are many examples of hydroxycarbonyl complexes that eliminate CO_2 to form metal hydrides or hydrogen.[36] Efforts to prepare **12** were unsuccessful, which prevented a direct evaluation of **12** as an intermediate. Two closely related platinum complexes, [Pt(PCP)(COOH)][21] and [Pt(PEt_3)$_2$(C_6H_5)(COOH)],[37] have been characterized by X-ray diffraction studies.[37] The latter complex and [Pt(PEt_3)$_2$(Cl)(COOMe)] are protonated in the presence of acid to form the corresponding carbonyl complexes and water or methanol.[37,38] On the other hand, [Pt(PEt_3)$_2$(Cl)(COOH)] reacts with water to form a hydride complex, [Pt(PEt_3)$_2$(Cl)(H)].[39]

The linear dependence of the catalytic current on acid concentration at low acid concentrations (Figure 6a) suggests a second-order dependence of the rate determining step on acid. Rapid deinsertion of CO_2 from **12** to form a hydride followed by protonation and elimination of hydrogen would be consistent with this observation. Another possible pathway is protonation of **12** to form hydrogen or CO. If protonation occurs at an oxygen atom, then decomposition leads to formation of CO. If protonation occurs at the Pd atom to form a hydride, then decomposition to form hydrogen could result. The hydrogen formed during electrolysis does not result from a [Pd(PCP)(CH_3CN)](BF_4) catalyzed water-gas shift reaction because CO and water do not produce CO_2 and H_2 in the presence of the catalyst and 0.025 M H_3PO_4 (i.e., under catalytic conditions). Clearly the nature of the tridentate ligand plays a major role in determining the reaction pathway. Under identical conditions, [Pd(PCP)(CH_3CN)](BF_4)$_2$ produces 100% H_2 while [Pd(etpC)(CH_3CN)](BF_4)$_2$ forms 98% CO,[25] although the catalytic currents for both complexes have the same dependence on CO_2 and acid.

Relationships between Ligand Structures and the Reactivity of Their Palladium Complexes with CO_2. One of the objectives of this study was to determine structure–activity relationships for [Pd(tridentate)(solvent)]$^{2+}$ molecules with respect to their ability to function as electrochemical CO_2 reduction catalysts. In particular we were interested in the relative importance of three factors: (1) the nature of the donor set of the tridentate ligand, (2) the bite size of the tridentate ligand, and (3) the basicity of the tridentate ligands as measured by the redox potentials of their corresponding palladium complexes. On the basis of the electrochemical studies discussed above, substitution of the central phosphorus atom with nitrogen or oxygen donors results in complexes for which no interaction with CO_2 is observed. Even the presence of a potential site for hydrogen bonding in [Pd(PNHP)(CH_3CN)](BF_4)$_2$ does not result in enhanced reactivity with CO_2 as reported for macrocyclic cobalt complexes.[40] Catalytic currents are observed for [Pd(PCP)(CH_3CN)](BF_4)$_2$, [Pd(PAsP)(CH_3CN)](BF_4)$_2$, and [Pd(PSP)(CH_3CN)](BF_4)$_2$ in the presence of both acid and CO_2. These currents are not observed in the absence of CO_2. Based on the relative magnitude of the catalytic currents the rates of reaction of Pd(I) intermediates with CO_2 appear to have the following qualitative order: PCP ≥ etp ≅ PAsP > ttp ≅ PSP > PNP, PNHP, POP. The rate of reaction of the Pd(I) intermediates with CO_2 does not follow the order of the trans influence for these ligands (ttp > PCP > etp > PAsP > PNP ≅ PNHP > PSP > POP) or the size of the chelate bite of the tridentate ligands (PNP ≅ PCP < POP ≅ PNHP < etp ≅ PSP ≅ PAsP < ttp). The observed order does roughly follow the order of the redox potentials for these complexes: PCP > etp ≅ PAsP ≅ ttp > PNP ≅ PNHP > POP ≅ PSP. On the basis of the data presented in this paper and the preceding paper[25] the optimal donor set for catalysts of the type [Pd(tridentate)(CH_3CN)](BF_4)$_2$ appears to be a simple triphosphine ligand. This is the only donor set for which we have observed reduction of CO_2 to CO.

Acknowledgment. This work was supported by the United States Department of Energy, Office of Basic Energy Sciences, Chemical Sciences Division.

Supplementary Material Available: Table 1s, containing crystal data, data collection conditions, and solution and refinement details for [Pd(PCP)(PEt_3)](BF_4), Tables 2s–6s, giving atomic coordinates and equivalent isotropic displacement parameters, bond lengths, bond angles, anisotropic displacement parameters, and hydrogen atom coordinates and isotropic parameters, Table 8s, containing crystal data, data collection conditions, and solution and refinement details for [Pd(PNP)(PEt_3)](BF_4)$_2$, and Tables 9s–13s, giving atomic coordinates and equivalent isotropic displacement parameters, bond lengths, bond angles, anisotropic displacement parameters, and hydrogen atom coordinates and isotropic parameters (28 pages). Ordering information is given on any current masthead page.

OM9403838

(36) Ford, P. C.; Rokicki, A. *Adv. Organomet. Chem.* **1988**, *28*, 139.
(37) Bennet, M. A.; Robertson, G. B.; Rokicki, A.; Wickramasinghe, W. A. *J. Am. Chem. Soc.* **1988**, *110*, 7098.
(38) Byrd, J. E.; Halpern, J. *J. Am. Chem. Soc.* **1971**, *93*, 1634.
(39) Clark, H. C.; Jacobs, W. J. *Inorg. Chem.* **1970**, *9*, 1229.
(40) Fujita, E.; Creutz, C.; Sutin, N.; Szalda, D. J. *J. Am. Chem. Soc.* **1991**, *113*, 343. Creutz, C.; Schwarz, H. A.; Wishart, J. F.; Fujita, E.; Sutin, N. *J. Am. Chem. Soc.* **1991**, *113*, 3361.